GEOPHYSICAL RESEARCH LETTERS, VOL. 37, L16706, doi:10.1029/2010GL044159, 2010

Is there regime behavior in monsoon convection in the late 20th century?

A. G. Turner[1] and A. Hannachi[2]

Received 31 May 2010; revised 8 July 2010; accepted 21 July 2010; published 25 August 2010.

[1] Mixture model techniques are applied to a daily index of monsoon convection from ERA-40 reanalysis to show regime behavior. The result is the existence of two significant regimes showing preferred locations of convection within the Asia/Western-North Pacific domain, with some resemblance to active-break events over India. Simple trend analysis over 1958–2001 shows that the first regime has become less frequent while the second becomes much more dominant. Both undergo a change in structure contributing to the total OLR trend over the ERA-40 period. Stratifying the data according to a large-scale dynamical index of monsoon interannual variability, we show the regime occurrence to be strongly perturbed by the seasonal condition, in agreement with conceptual ideas. This technique could be used to further examine predictability issues relating the seasonal mean and intraseasonal monsoon variability or to explore changes in monsoon behavior in centennial-scale model integrations. **Citation:** Turner, A. G., and A. Hannachi (2010), Is there regime behavior in monsoon convection in the late 20th century?, *Geophys. Res. Lett.*, *37*, L16706, doi:10.1029/2010GL044159.

1. Introduction

[2] The Asian summer monsoon affects the lives of more than one-third of the world's population for their water supply for industry, agriculture and human habitation. While large-scale drivers of the seasonal mean monsoon are relatively well understood through low frequency variations in the lower boundary forcing such as the El Niño Southern Oscillation [*Charney and Shukla*, 1981], the relationship between modes of monsoon intraseasonal variability (MISV) and the overall seasonal mean is unclear. MISV on timescales of approximately 30–60 days reveals itself in increased and deficient precipitation over a given monsoon region, known colloquially as *active* and *break* events, which can have a dramatic impact on agriculture. Northward propagations of MISV are often associated with the eastward propagating summertime Madden-Julian Oscillation [*Sperber and Annamalai*, 2008].

[3] The null hypothesis would suggest an increased intensity or frequency of active conditions during strong monsoon summers, and more frequent breaks during drought years. Indeed *Palmer* [1994] envisaged a chaotic Lorenz model in which the probability of lying in either the active or break regime is influenced by the lower boundary forcing. However, no straightforward demonstration of this idea has been depicted in observed or model data until now. For example, *Sperber et al.* [2000] showed that only a small subset of MISV (represented by particular principal components beyond the leading mode) could be perturbed by large scale forcing. *Straus and Krishnamurthy* [2007] have also shown evidence to suggest bimodality under certain conditions. Other authors have suggested that seasonal mean monsoon rainfall is the sum of a large-scale externally forced component and the statistics of MISV during the season which are largely unpredictable [*Krishnamurthy and Shukla*, 2000, 2007]. Thus it is unclear whether the large-scale drives intraseasonal variability, or whether it is itself determined by MISV.

[4] This study applies mixture model techniques (as employed by *Hannachi and Turner*, 2008 and *Woollings et al.* [2010]) to a simple index of Asian monsoon convection derived from the ERA-40 reanalysis, to show that preferred regimes of convection can be related to the large scale. Section 2 describes the datasets and indices used and the mixture model technique. Results are discussed in section 3 while the implications are considered in section 4.

2. Method

2.1. Data Used

[5] We use the ECMWF reanalysis ERA-40 [*Uppala et al.*, 2005] for daily outgoing longwave radiation (OLR) and lower tropospheric (850 hPa) winds over the period 1958–2001 on a Gaussian grid of approximately 1.125° spacing. Monthly anomalies are generated in these fields by removing the seasonally varying mean from each month. OLR is a good proxy for convection and precipitation in the tropics. In addition, as an independent measure of rainfall over India, we use the India Meteorological Department one degree gridded product [*Rajeevan et al.*, 2006] based on spatial averages of 2140 stations each day since 1951. We curtail this dataset to match the ERA-40 period.

2.2. Mixture Model

[6] Following previous works [*Hannachi and Turner*, 2008; *Woollings et al.*, 2010] we use a mixture model technique (described in more detail by *Hannachi and O'Neill* [2001] and *Hannachi* [2007]) to examine the probability distribution of monsoon convection over the ERA-40 period. This follows the result that any multivariate probability density function (pdf) $f(\mathbf{x})$ may be decomposed as a weighted sum of multivariate Gaussians [*Anderson and Moore*, 1979] as in:

$$f(\mathbf{x}) = \sum_{k=1}^{c} \alpha_k g_k(\mathbf{x}, \boldsymbol{\Sigma}_k, \boldsymbol{\mu}_k) \quad (1)$$

[1]NCAS-Climate, Walker Institute for Climate System Research, Department of Meteorology, University of Reading, Reading, UK.
[2]Department of Meteorology, University of Reading, Reading, UK.

0094-8276/10/2010GL044159

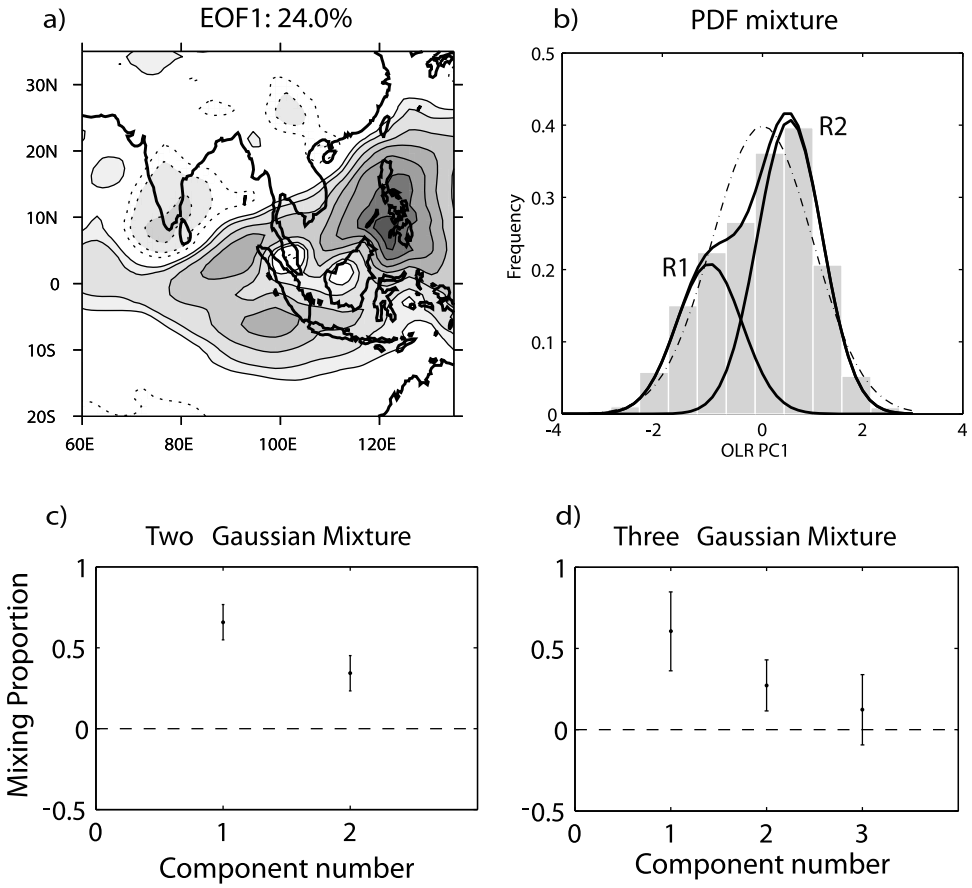

Figure 1. (a) Loading pattern of the leading mode of variability of JJAS OLR anomalies calculated by EOF analysis in the ERA-40 data over 1958–2001. Positive (negative) contours are dotted (solid). (b) Distribution of the daily OLR index (upper solid line) and those of it two significant mixture components (beneath, indicated R1, 2 for clarity). A Gaussian normal is also shown (dashed). Mixing proportions for (c) two- and (d) three-Gaussian mixtures in the whole period, showing 1% confidence intervals.

where $\alpha_1, \ldots, \alpha_c$ are the mixing proportions which satisfy:

$$0 < \alpha_k < 1 \text{ for all } \alpha \text{ and } \sum_{k=1}^{c} \alpha_k = 1, \qquad (2)$$

and $\boldsymbol{\mu}_k$ and $\boldsymbol{\Sigma}_k$ are the mean and covariance matrix respectively of the kth multivariate Gaussian $g_k(\mathbf{x})$. The number of Gaussians is increased until significance is no longer attained.

2.3. Indices Used

[7] We define the dominant mode of variability in summertime (June–September; JJAS) convection over the Asian and Western North Pacific (WNP) summer monsoon regions as the first latitude-weighted empirical orthogonal function (EOF) of monthly OLR anomalies from ERA-40. This is calculated over the domain 60–135°E, 20°S–35°N and its loading pattern is shown in Figure 1a. This mode explains around 24% of the variance in OLR, well distinct from the remaining higher order modes (the second mode explains only ~12% variance). The largest signal in Figure 1a is a southwest-northeast oriented band over the Maritime Continent, while a slightly weaker center of opposite sign is found over India. Note that this leading mode emerges irrespective of linear detrending being performed on the data. Various other domains were tested with no significant bearing on the relative fraction explained by the first mode nor on the dominance of the WNP. The daily OLR anomaly was projected onto the loading pattern by performing a simple linear regression, using the regression coefficient at each day. After being normalized by its standard deviation, this forms the daily index of monsoon convection.

[8] As an independent measure of the large-scale seasonal mean monsoon, we employ a dynamical index of *Webster and Yang* [1992, hereafter WY], defined as the June to September average anomalous zonal windshear between lower (850 hPa) and upper (200 hPa) tropospheric winds. This is averaged over the broad 40–110°E, 5–20°N Asian monsoon region and well represents heating in the atmospheric column.

3. Results

3.1. Regimes of Convection

[9] The distribution of the daily index x_t (t = 1…5368) is shown in Figure 1b (upper solid line) and is quite distinct from the normal distribution, containing a notable shoulder in the negative side, which suggests the existence of two preferred centers. The skewness of this data is strong at −0.30. The mixture model technique outlined above is applied to the daily OLR index yielding only two Gaussian

components with significance higher than the 1% level (Figures 1c and 1d), with mixing proportions of 0.34 and 0.66 centered at -1.06σ and 0.55σ respectively, as shown also in Figure 1b.

[10] Weightings, or membership probabilities, for each regime as a function of time can be computed following

$$w_k(t) = \alpha_k g_k(t)/c(t) \tag{3}$$

for $k = 1, 2$ where

$$g_k(t) = \exp\left(-\left((\mu_k - x_t)^2\right)/(2\sigma_k)\right)/\sqrt{2\pi\sigma_k}, \tag{4}$$

and

$$c(t) = \alpha_1 \exp\left(-\left((\mu_1 - x_t)^2\right)/(2\sigma_1)\right)/\sqrt{2\pi\sigma_1} + \alpha_2 \exp\left(-\left((\mu_2 - x_t)^2\right)/(2\sigma_2)\right)/\sqrt{2\pi\sigma_2}, \tag{5}$$

where the subscripts 1 and 2 represent the first and second regimes respectively, and x_t ($t = 1 \ldots 5368$) is our daily JJAS OLR timeseries. Composites of various atmospheric fields can then be calculated. Reconstructed regime composites of OLR anomalies to the seasonal cycle (Figures 2a–2d) well match the negative and positive phases of EOF1 in Figure 1 for the first and second regimes respectively. The centers have magnitudes of approximately ±10 W m^{-2} over southern India and ±20 W m^{-2} over the Philippines. Figures 2a and 2c also show composite lower tropospheric (850 hPa) wind anomalies self-consistent with the OLR field and the dominance of activity over the South China Sea. There is also clear evidence of a southward deviation in the Somali Jet in regime 2 (Figure 2c), consistent with the increased OLR and negative precipitation anomalies over peninsular India (Figure 2d). This deviation leads to strong anomalous convergence, and consequently enhanced convection, over the eastern equatorial Indian Ocean as observed during break conditions over India [*Krishnan et al.*, 2000]. Although there is some resemblance to active and break conditions in the Indian monsoon, we note that observed signals generally dominate over the central India core monsoon region [*Rajeevan et al.*, 2010]. The much larger domain used here instead reveals the dominance of the WNP region.

[11] To confirm that these regimes are not simply an artifact of the mixture model, we also employed a physically-based method of sorting the daily data to further support our case, as in *Woollings et al.* [2010]. A daily index of the strength of the WNP monsoon devised by *Wang and Fan* [1999] and defined as the normalised difference between zonal lower tropospheric winds in the southern (100–130°E, 5–15°N) and northern (110–140°E, 20–30°N) WNP, is used to partition the daily OLR timeseries into strong and weak days (not shown). Such an analysis reveals distributions analogous to the mixture model-derived functions in Figure 1b, although the relative probabilities are slightly different. Such comparisons will be explored in detail, along with indices for the Indian region, in a further work.

3.2. Regime Trends over the ERA-40 Period

[12] To analyse any possible trend in regime behavior over the ERA-40 period, we split the timeseries into two parts, 1958–1975 and 1979–2001. Although not equal in length, these represent periods prior to and following the climate shift observed in the Indo-Pacific in 1976/77 [e.g. *Turner et al.*, 2007]. The mixture model analysis was repeated for each period and two-component mixtures are shown in Figure 3a. While both periods support two distinct regimes, significance of the mixture falls to 95% in the later period. If the OLR timeseries is first linearly detrended, then regimes in the second period are significant only at the 90% level. There is also a clear change in skewness, from 0.15 to −0.13, already suggesting that the relative dominance of the regimes is changed. The change over the ERA-40 period is quite dramatic, the first component of the early period being substantially inhibited during the second period, whilst the second regime becomes much more frequent. The consequent impact of the trend in regime behavior on composites of OLR, 850 hPa wind and Indian rainfall is shown in Figures 2e–2h. The main feature is a negative trend in OLR over the Maritime Continent in both regimes, associated with local cyclonic anomalies, and anticyclonic anomalies further north. Examination of the raw ERA-40 OLR and independent data from NCEP-NCAR reanalysis (not shown) suggests that Figures 2e and 2g are in qualitative agreement with general trends in OLR in the WNP region. The response over India (Figures 2f and 2h) is rather mixed, with reductions in rainfall (and increased OLR) over the north and Western Ghats, consistent with a weakened Somali Jet. In regime 2, there are increases in rainfall over the central-eastern peninsula owing to convergence of moist air from the Bay of Bengal. This inhomogeneous response is consistent with that of *Goswami et al.* [2006] who noted no clear trend in the observed record over India. We note that trends in higher order modes not included in the index may play a role.

3.3. Relationship with the Seasonal Mean Monsoon

[13] To determine if there is a relationship between the large-scale, seasonal mean monsoon and short timescale variability, our OLR index is stratified according to the JJAS-average Webster-Yang (WY) index outlined in section 2.3. The mixture model analysis is repeated for each subset, and displayed in Figure 3b. This clearly suggests rather different regime behavior under WY+ and WY− conditions: seasons with strong broad-scale monsoon heating possess approximately equal likelihoods of each regime, while the second regime (break conditions over India) becomes much more frequent during WY−. These stark results extend the findings of *Sperber et al.* [2000] and support Palmer's hypothesis [*Palmer*, 1994], that the seasonal mean condition relates to preference for a particular weather regime. This implies the possibility of enhanced predictability of monsoon conditions on seasonal and weekly timescales. Analysis of the relationship with the seasonal mean in the context of long-term trends will be addressed in a subsequent paper.

4. Summary and Conclusions

[14] By using statistical mixture model methods on a simple daily index of convection we have demonstrated evidence for two preferred regime structures in Asian monsoon convection. These are found to be dominated by coherent convection and circulation structures over the WNP, although signals extend to the Indian monsoon domain where deviation in the Somali Jet and associated low-level divergence partially resembles break conditions over the peninsula. A

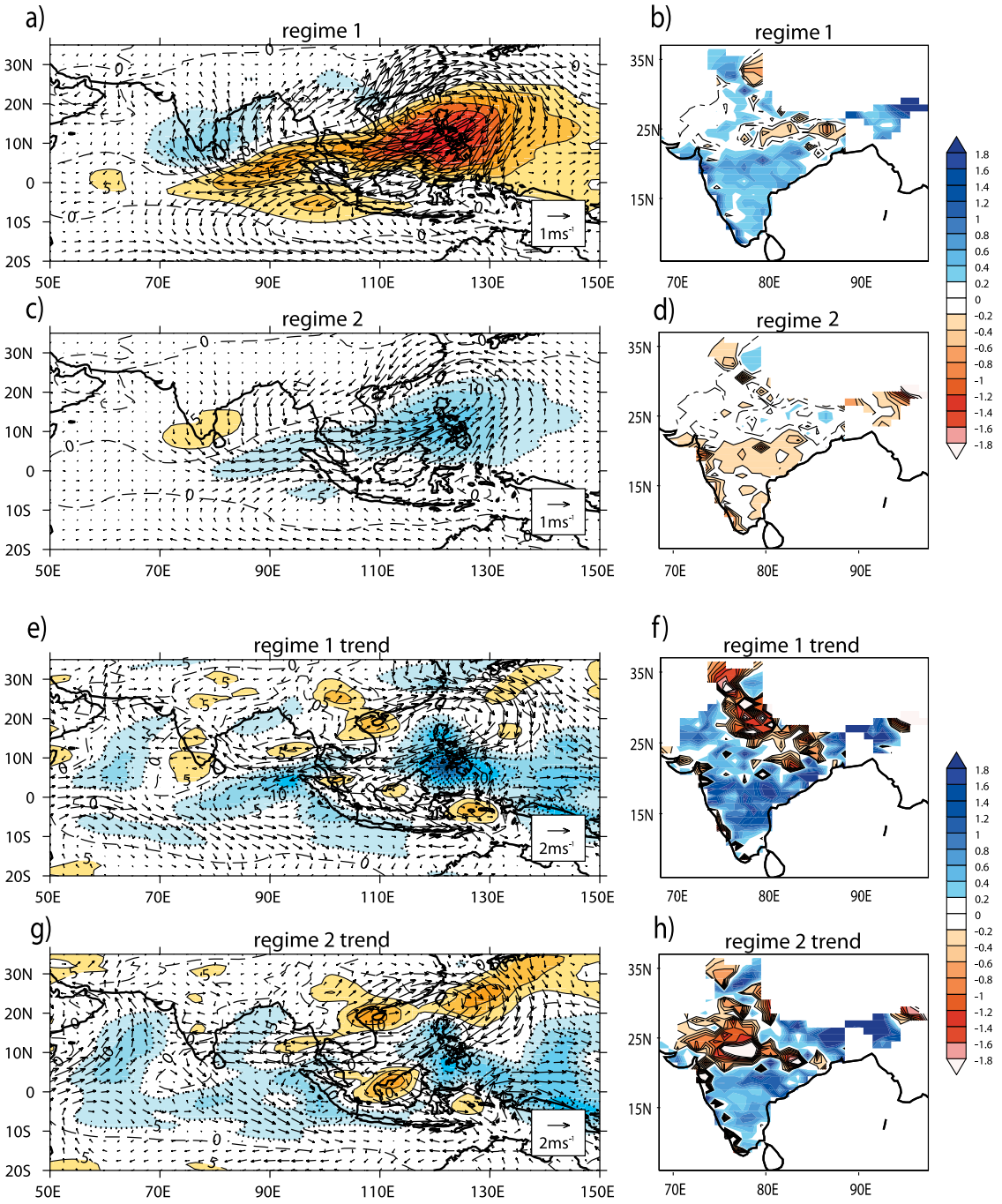

Figure 2. Composite anomalies of OLR with 850hPa wind and rainfall over India in the (a, b) first and (c, d) second regimes over the whole 1958–2001 period. Late minus early period difference in the (e, f) first and (g, h) second regimes. Contour interval for OLR composites is 5 W m^{-2}, red solid (blue dotted) is positive (negative). Rainfall units are mm/day, negative contour lines only are shown.

notable and significant trend is found in the regime probability and structure over the recent observed record, in particular suggesting shifts in the regime structure which are strongly evident in the observed trend in raw OLR data. The much less frequent first regime suggests less regime behavior in recent years. Finally, by stratifying the data according to a large-scale index of seasonal mean monsoon heating, we have demonstrated a strong relationship between the seasonal mean and its intraseasonal behavior, in support of Palmer's hypothesis. Indeed the dominance of one regime over another dramatically increases under weak seasonal mean monsoon heating conditions. Following *Sperber et al.* [2000] and results of *Straus and Krishnamurthy* [2007], this suggests additional predictability of intraseasonal monsoon convection may be possible according to large-scale conditions. We have not yet explored the link between lower boundary forcings such as ENSO and the regime behavior that would elucidate this enhanced predictability. Further examination is required of this technique, perhaps by incorporating higher order modes of variability into the monsoon

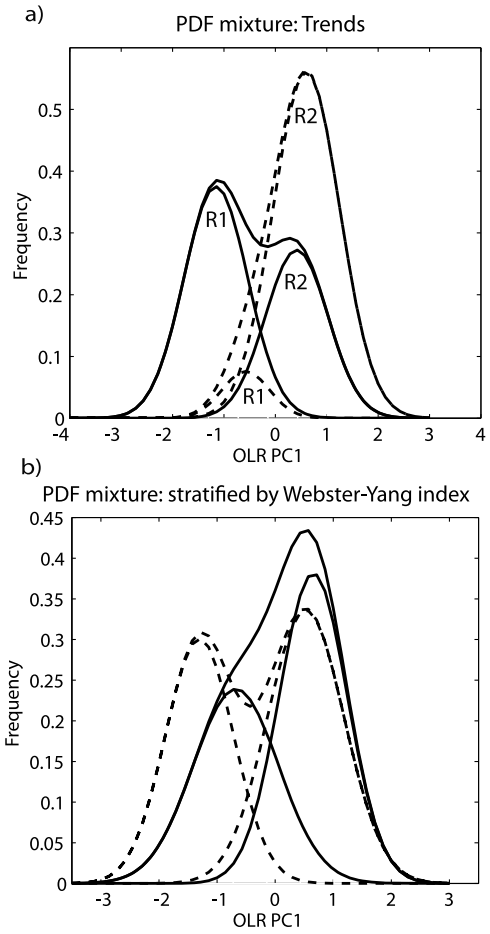

Figure 3. (a) Pdfs of the daily OLR index in the early (solid) and late (dashed) part of the dataset. Upper (lower) curves represent total (mixture) distributions. Regimes are indicated R1,2 for clarity. (b) Perturbations to the whole period mixture when stratified by the JJAS-average Webster-Yang monsoon index: WY+ (dashed) and WY− (solid).

index [e.g. as in *Molteni et al.*, 2003] in order to capture more fully the spatio-temporal variability representative of the monsoon, thus also allowing a more complete analysis of trends in the regimes. This methodology offers the potential to examine internally forced changes to regime behavior in long integrations of coupled climate models, now that some are able to simulate the appropriate mean state conditions and propagation characteristics associated with MISV [*Sperber and Annamalai*, 2008].

[15] **Acknowledgments.** AG Turner was supported via the National Centre for Atmospheric Science—Climate directorate, a collaborative center of the Natural Environment Research Council.

References

Anderson, B. D., and J. B. Moore (1979), *Optimal Filtering*, Prentice Hall, Englewood Cliffs, N. J.

Charney, J. G., and J. Shukla (1981), *Monsoon Dynamics: Predictability of Monsoons*, edited by J. Lighthill and R. Pearce, Cambridge Univ. Press, Cambridge, U. K.

Goswami, B. N., V. Venugopal, D. Sengupta, M. S. Madhusoodanan, and P. K. Xavier (2006), Increasing trend of extreme rain events over India in a warming environment, *Science*, *314*, 1442–1445, doi:10.1126/science.1132027.

Hannachi, A. (2007), Tropospheric planetary wave dynamics and mixture modelling: Two preferred regimes and a regime shift, *J. Atmos. Sci.*, *64*, 3521–3541, doi:10.1175/JAS4045.1.

Hannachi, A., and A. O'Neill (2001), Atmospheric multiple equilibria and non-Gaussian behaviour in model simulations, *Q. J. R. Meteorol. Soc.*, *127*, 939–958, doi:10.1002/qj.49712757312.

Hannachi, A., and A. G. Turner (2008), Preferred structures in large scale circulation and the effect of doubling greenhouse gas concentration in HadCM3, *Q. J. R. Meteorol. Soc.*, *134*, 469–480, doi:10.1002/qj.236.

Krishnamurthy, V., and J. Shukla (2000), Intraseasonal and interannual variability of rainfall over India, *J. Clim.*, *13*, 4366–4377, doi:10.1175/1520-0442(2000)013<0001:IAIVOR>2.0.CO;2.

Krishnamurthy, V., and J. Shukla (2007), Intraseasonal and seasonally persisting patterns of Indian monsoon rainfall, *J. Clim.*, *20*, 3–20, doi:10.1175/JCLI3981.1.

Krishnan, R., C. Zhang, and M. Sugi (2000), Dynamics of breaks in the Indian summer monsoon, *J. Atmos. Sci.*, *57*, 1354–1372, doi:10.1175/1520-0469(2000)057<1354:DOBITI>2.0.CO;2.

Molteni, F., S. Corti, L. Ferranti, and J. M. Slingo (2003), Predictability experiments for the Asian summer monsoon: Impact of SST anomalies on interannual and intraseasonal variability, *J. Clim.*, *16*, 4001–4021, doi:10.1175/1520-0442(2003)016<4001:PEFTAS>2.0.CO;2.

Palmer, T. N. (1994), Chaos and predictability in forecasting the monsoons, *Proc. Indian Natl. Sci. Acad.*, *60*, 57–66.

Rajeevan, M., J. Bhate, J. D. Kale, and B. Lal (2006), High resolution daily gridded rainfall data for the Indian region: Analysis of break and active monsoon spells, *Curr. Sci.*, *91*, 296–306.

Rajeevan, M., S. Gadgil, and J. Bhate (2010), Active and break spells of the Indian summer monsoon, *J. Earth Syst. Sci.*, *119*, 229–247.

Sperber, K. R., and H. Annamalai (2008), Coupled model simulations of boreal summer intraseasonal (30–50 day) variability, Part 1: Systematic errors and caution on use of metrics, *Clim. Dyn.*, *31*(2–3), 345–372, doi:10.1007/s00382-008-0367-9.

Sperber, K. R., J. M. Slingo, and H. Annamalai (2000), Predictability and the relationship between subseasonal and interannual variability during the Asian summer monsoon, *Q. J. R. Meteorol. Soc.*, *126*, 2545–2574, doi:10.1002/qj.49712656810.

Straus, D., and V. Krishnamurthy (2007), The preferred structure of the interannual Indian monsoon variability, *Pure Appl. Geophys.*, *164*, 1717–1732, doi:10.1007/s00024-007-0248-x.

Turner, A. G., P. M. Inness, and J. M. Slingo (2007), The effect of doubled CO_2 and model basic state biases on the monsoon-ENSO system. II: Changing ENSO regimes, *Q. J. R. Meteorol. Soc.*, *133*, 1159–1173, doi:10.1002/qj.83.

Uppala, S. M., et al. (2005), The ERA-40 re-analysis, *Q. J. R. Meteorol. Soc.*, *131*(612), 2961–3012, doi:10.1256/qj.04.176.

Wang, B., and Z. Fan (1999), Choice of South Asian summer monsoon indices, *Bull. Am. Meteorol. Soc.*, *80*, 629–638, doi:10.1175/1520-0477(1999)080<0629:COSASM>2.0.CO;2.

Webster, P. J., and S. Yang (1992), Monsoon and ENSO—Selectively interactive systems, *Q. J. R. Meteorol. Soc.*, *118*(507), 877–926, doi:10.1002/qj.49711850705.

Woollings, T., A. Hannachi, B. Hoskins, and A. G. Turner (2010), A regime view of the North Atlantic Oscillation and its response to anthropogenic forcing, *J. Clim.*, *23*, 1291–1307, doi:10.1175/2009JCLI3087.1.

A. Hannachi, Department of Meteorology, University of Reading, PO Box 243, Earley Gate, Reading RG6 6BB, UK. (a.hannachi@reading.ac.uk)

A. G. Turner, NCAS-Climate, Walker Institute for Climate System Research, Department of Meteorology, University of Reading, PO Box 243, Earley Gate, Reading RG6 6BB, UK. (a.g.turner@reading.ac.uk)